
Proceedings Paper:
Soto, C., Sims, N.D., Ozturk, E. et al. (1 more author) (2024) Unsupported machining fixture layout optimisation. In: Journal of Physics: Conference Series. XII International Conference on Structural Dynamics, 03-05 Jul 2023, Delft, Netherlands. IOP Publishing .

https://doi.org/10.1088/1742-6596/2647/2/022006

Unsupported machining fixture layout optimisation

Journal of Physics: Conference Series **2647** (2024) 022006 doi:10.1088/1742-6596/2647/2/022006

Unsupported machining fixture layout optimisation

C Soto[1,2], N D Sims [1], E Ozturk[1] and B Weekes[2]

[1] Industrial Doctorate Centre in Machining Science, The University of Sheffield, Sir Frederick Mappin Building, Mappin Street, Sheffield S1 3JD, UK

[2] GKN Aerospace, Global Technology Centre, Taurus Rd, Patchway, Filton, Bristol BS34 6FB, UK

E-mail: c.soto@sheffield.ac.uk

Abstract. It is well established that excessive vibrations in machining operations hinder productivity and quality of the components being made. In these environments it is common to encounter self-excited vibrations due to the dynamic response characteristics of the cutting tool and workpiece; referred to as regenerative chatter. To suppress these effects, conventional practices provide the workpiece with as much support as possible and therefore commonly require custom-built fixturing bases and several manual intervention stages. In contrast, for modern reduced fixturing approaches, the workpiece is minimally-held, with the benefits of reduced setup times, lower fixturing and inventory costs, and improved access to the workpiece thereby avoiding multi-stage setups. However, minimal fixturing reduces support of the workpiece, and so vibration becomes a greater challenge, along with the subsequent detrimental effects to part quality and material removal rate (MRR). This paper sets out to determine an optimisation methodology for layout configurations that maximise milling depths of cut whilst achieving dynamic stability; by means of FEA model-based simulations and particle swarm optimisation (PSO) methods. The optimisation algorithm is then tested on simplified setups and compared to exhaustive searches. It is shown that optimal results can differ from standard practice, and despite the comparative reduction in workpiece stiffness to a traditional approach is mostly unavoidable, careful placement of workholding elements can reportedly improve cutting conditions and increase dynamic stability within an unsupported environment.

1 Introduction

Designing and building machining fixtures are critical tasks for aerospace manufacturing companies, particularly when dealing with large scale double-sided components. These fixtures need to ensure reliable and repeatable alignment whilst providing sufficient clamping force which commonly results in stage specific bases and bespoke solutions. The downsides of using these methods include significant development and operational costs, as well as limited versatility to handle varied geometries within a family of parts. Modern tendencies in large thin-walled components are looking at single setup environments which can allow unrestricted access to the workpiece on both sides [1], referred to as double sided access (DSA), schematic shown in Figure 1. The main challenge arising from this ambitious type of setup is an increase in machining induced vibrations issues due to the inherent reduction in workpiece stiffness.

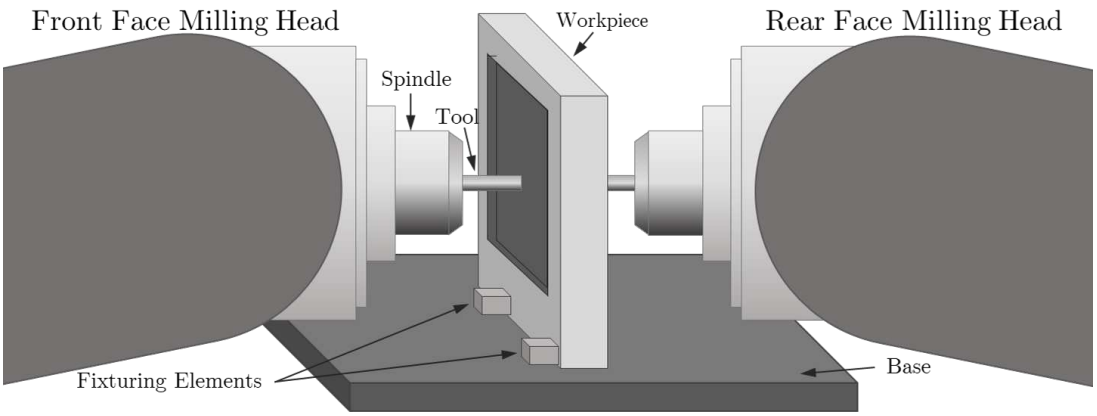

Figure 1: Schematic drawing of a DSA setup.

Given that the dynamic response of the workpiece is directly related to its holding configuration, this paper looks at improving the understanding of the effects different layouts have on the dynamic response and to develop an optimisation routine to derive the best layout under a series of conditions. This intends to provide DSA fixtures with enhanced and competitive productivity compared to traditional workholding methods. It also serves as a bridge between the fields of machining dynamics and fixture layout optimisation, which have seen few studies linking them together [2]. The ultimate aim is to deveop an integrated system of computer-aided fixture design using FEA dynamic analysis to derive optimal clamping positions which maximise stable depth of cut.

2 Machining Overview

2.1 Machining dynamics

A common objective in machining is to maximise the material removal rate (MRR) of a given tool path. For milling operations it is defined as:

$$\text{MRR} = a_p a_e f_t N_t \Omega \tag{1}$$

Where a_p and a_e are the axial and radial depths of cut respectively, and f_t, N_t and Ω are the feed per tooth, number of teeth and spindle speed of the tool (see Figure 2). The term of interest in this work is the stable limit for the axial depth of cut, $a_{p,lim}$, which is dependant on the transfer function of the system following the generic expressions [3, 4]:

$$a_{p,lim} = \frac{-1}{2K_f G(f_c)} \tag{2}$$

$$\frac{f_c}{\Omega} = N + \frac{\varepsilon}{2\pi} \tag{3}$$

$G(f_c)$ is the real valued part of a driving point receptance in the system, K_f is a cutting force constant, whilst f_c is the chatter frequency. N is the *lobe number*, and quantifies the integer number of oscillations between current and previous tooth paths whilst ε is the phase between them. These expressions state the relationship between the system's dynamic response and the stable axial depth of cut limit. Given that a_p is a physical quantity, the negative valued part of the real transfer function is required. The inverse relationship also showcases that flexible

structures will reduce the axial depth of cut and eventual productivity, as well as harder materials that exhibit a larger K_f value.

When plotting the axial depth of cut against the tool spindle speed for a number of values of N, a *Stability Lobe Diagram* (SLD) is generated. As seen in Figure 3, a representative single degree of freedom FRF is related to the SLD plot at different points. These SLD plots give a valuable guideline to machinists, by relating the tool spindle speed (Ω) and its axial depth of cut (a_p) to the chatter stability. If a pair of speed and depth parameters lie underneath the boundary lines of each lobe, it is deemed to be a stable cut with no chatter. On the contrary, points that fall over the boundary are unstable and chatter is expected. The critical depth of cut, $a_{p,crit}$, defines a limit under which no chatter is expected irrespective of spindle speed, and corresponds to the frequency at the minimum point of the real-valued FRF.

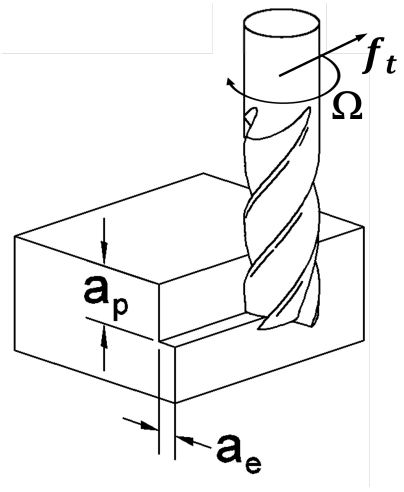

Figure 2: Milling process parameters.

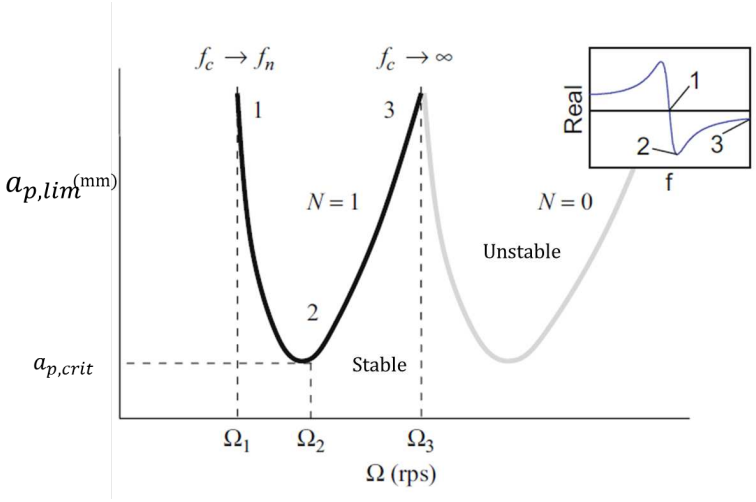

Figure 3: Example SLD plot for N={0,1}, relating points on the real part FRF of the system to the SLD, from [4].

Given that boundary conditions have a direct influence on the equations of motion of the system, and therefore determine the mode shapes and natural frequencies, the aim of this research is to develop an automated program that can optimise the location of work-holding elements and increase the stable depth of cut limit.

2.2 Computer assisted fixture design (CAFD)

Using computational tools to enhance fixture designs is a field that has seen developments in both assembly and manufacturing applications. Focusing on machining, the minimum requirements expected out of a fixture are the location and clamping, for accurate positioning of the part and sufficient support for its machining operations [5]. Nevertheless, a series of additional capabilities have been developed with the aid of computational evaluation [2] and this has enabled optimisation efforts targeting a range of aspects including part displacements, cooling, vibration suppression, and others.

Most of the vibration suppression work has been centered around ancillary devices that attach to flexible, or re-configurable, fixtures in order to provide higher damping properties by means of tuned mass dampers, particle based dampers and eddy current damping [6]. Few studies have directly targeted workholding layouts with vibration avoidance as a key metric [7]. These

articles also target single-sided bespoke and conforming fixtures, leaving an opportunity to evaluate layout optimisation in double-sided and picture-frame type solutions.

3 Layout Optimisation

The starting point for the development of a optimisation routine targeting double-sided fixturing solutions is evaluating a rectangular billet with clamps placed along its external edges. The characteristic of these can vary as part of the manipulated variable within the solver.

All variables, constraints and requirements the optimisation protocol are derived from three main areas:

- **Physical** requirements that define the geometrical aspects of the system: billet shape and size, number of clamps or vices and their dimensions, type of material to evaluate, etc.
- **FEA** dynamic evaluations where the simulation of the physical setup is performed. It defines meshing parameters, subdivision of node/element sets, boundary conditions, damping, joint parameters and model updating.
- **Numerical computation** is in charge of all evaluation instances and scripting procedures, serving as the backbone and linkage hub for all areas. It uses constraints defined by the physical setup and FEA environments to evaluate different approaches. It also defines the parametrisation of the layout deriving in the combinatorial search space of possible layouts.

3.1 Layout parametrisation

A simplified combinatorial analysis of the total amount of possible layouts (Γ_T) for N equal vices can be defined using the nomenclature shown in Figure 4. The total amounts of positions a vice of length l_i can occupy on all j sides of the billet is:

$$P_T = \sum_j \left\lfloor \frac{\bar{L_j}}{\Delta l} + 1 \right\rfloor \in \mathbb{N} \tag{4}$$

Where $\bar{L_j}$ and Δl are the indexable length and the spatial resolution respectively. However, considering the disabled space a clamp takes up on the next one (u), gives:

$$u = 2\left\lfloor \frac{l_i}{\Delta l} \right\rfloor - 1 \tag{5}$$

Which leads to the possible number of layouts being:

$$\Gamma_T = \prod_{i=1}^{N} \Big(P_T - u(i-1) \Big) \tag{6}$$

Inserting (4) and (5) into eq. (6) gives:

$$\therefore \Gamma_T \propto \left(\frac{L_j - 2l_i}{\Delta l} \right)^N \tag{7}$$

Equation 7 highlights how quickly the total number of layouts can grow when refining the spatial resolution or increasing the number of billets. As a quick numerical example, a rectangular billet of dimensions (500×700)mm, with $N = 4$ vices of length, $l_i = 100$mm, at $\Delta l = 10$mm result in over $9 \cdot 10^8$ possible layouts.

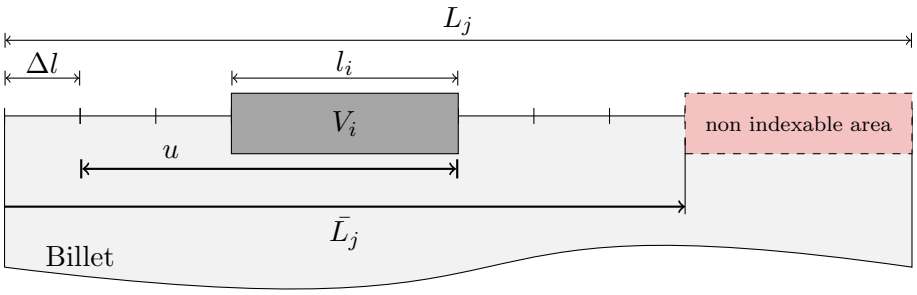

Figure 4: Definition of parameterisation variables

3.2 Optimisation fitness and objective functions

The complete search space of possible layouts is impractical to evaluate exhaustively unless severe simplifications are made. This encourages the development of an optimisation program that can speed-up the process of finding the most suitable layout. Nevertheless what constitutes a *suitable* layout requires strict definition as a fitness and objective function.

As seen in equations 1 and 2 the direct dependence on the real part of a driving point FRF is paramount in order to avoid regenerative chatter. The proposed fitness function in this case is to evaluate the *minimum value of the real part FRF* within a specified frequency range. An evenly spaced rectangular grid across the workpiece provides the set of evaluation points (k) where FRFs in the three main directions are extracted. With this, the objective function can be defined as:

$$\max_{\Gamma_i} \quad \min_{k,\omega_c} G_k(\omega_c) \tag{8}$$

This optimisation formula evaluates an arbitrary layout (Γ_i) by selecting the minimum value of the real part FRF within the evaluation points on the component (G_k). By comparing this value over a set of layouts, the optimal is that which has the largest minimum real part FRF. This approach is independent of tooling and cutting parameters, as it bases all calculations strictly on the dynamic response of the workpiece.

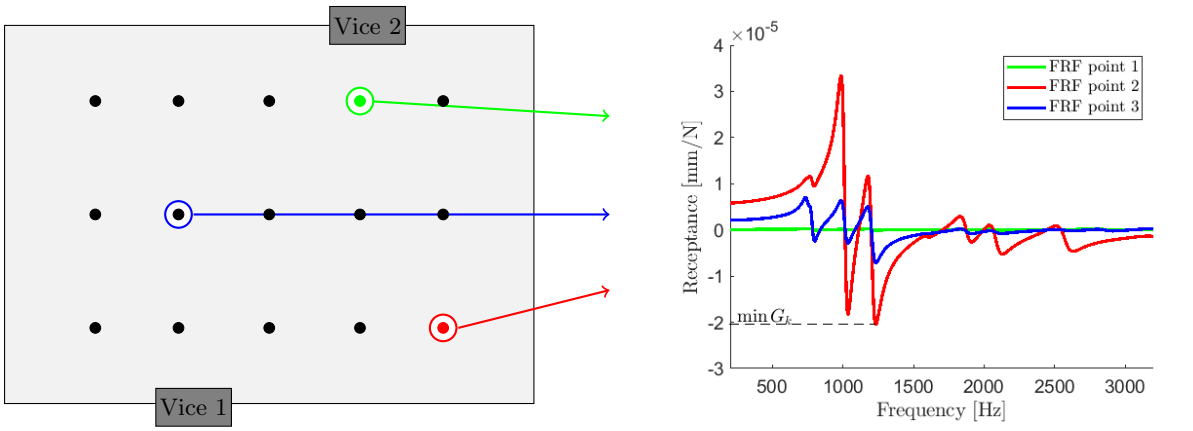

(a) Evaluation points on workpiece

(b) Example FRF from 3 driving points in $\hat{k}$

Figure 5: Example of FRF extraction from (a) evaluation points and (b) real FRF plot

3.3 Optimisation algorithm

In this instance a *particle swarm optimisation* (PSO) approach is chosen as it is well documented metaheuristic that has been useful in other developments within machining fixture layout optimization (MFLO) research [8].

The initialisation of the system considers a selection of layout particles randomly generated within the search space. Additionally, a velocity vector is associated to each layout seed to define the direction in which subsequent generations are set to travel. These vectors can be defined as:

$$\Gamma_i = (x_{i1}, x_{i2}, ..., x_{in}) \quad x_{ij} \in [0, \bar{L_T}] \tag{9}$$

$$\dot{\Gamma}_i = (v_{i1}, v_{i2}, ..., v_{in}) \quad v_{ij} \in [-V_{max}, V_{max}] \tag{10}$$

For every generation the objective function must be evaluated for each particle, which requires an FE model to export the FRFs and modal parameters. After evaluating the exported results from the FE software, the four parameters from the PSO approach are stored, namely:

- P_i, the vector array containing the best position for each particle for all generations.
- P_{best}, the value of the fitness function for each position of P_i.
- P_g, the single overall best particle position for the entire swarm. $P_g \in P_i$
- g_{best}, the single overall best fitness function value for the entire swarm. $g_{best} \in P_{best}$

The first two PSO parameters (P_i and P_{best}) are defined for each particle of the swarm. As the generations progress, these arrays are evaluated and updated to compare the evolution any individual particle has had. The next two PSO parameters are defined for the entirety of the swarm, defining the best overall position (P_g) and best overall fitness function value (g_{best}). Once these parameters have been stored for a given generation, the particles new position is updated following the expressions:

$$\dot{\Gamma}_i(t+1) = \dot{\Gamma}_i(t) + C_1 r_1 (P_i - \Gamma_i(t)) + C_2 r_2 (P_g - \Gamma_i(t)) \tag{11}$$

$$\Gamma_i(t+1) = \Gamma_i(t) + \dot{\Gamma}_i(t+1) \tag{12}$$

The speed of the particle contains three main terms: the first is the "*inertia or momentum*" as the tendency to travel in the same initial direction. The second, "*memory or nostalgia*", attracts the particle to its own best experience. And the third term, the"*cooperation or shared information*", attracts the particle towards the best global experience of all particles. The constants C_1 and C_2 are positive weighting factors for the randomized coefficients r_1 and r_2 which are uniformly distributed in the $[0, 1]$ interval. The implementation procedure is detailed in [9] and also surveys studies that have evaluated the performance of a PSO using linear and non-linear rules to dynamically change the weighting of the inertia. Upon inspection of results and performance of the search algorithm, weighting of the inertia component can be explored.

3.4 Software implementation

A soft computing program is scripted to link both the FEA platform, FEMTOOLS 4.20, and updating the PSO parameters. This main compiling algorithm is generated in MATLAB, workflow of which can be depicted in Figure 6. All simulations are performed on a DELL workstation (Intel Xeon 3.0GHz CPU, 16GB RAM).

User defined variables initialise the optimisation program by determining physical constraints on the number and length of vices, the billet's size, material properties and edge availability, as

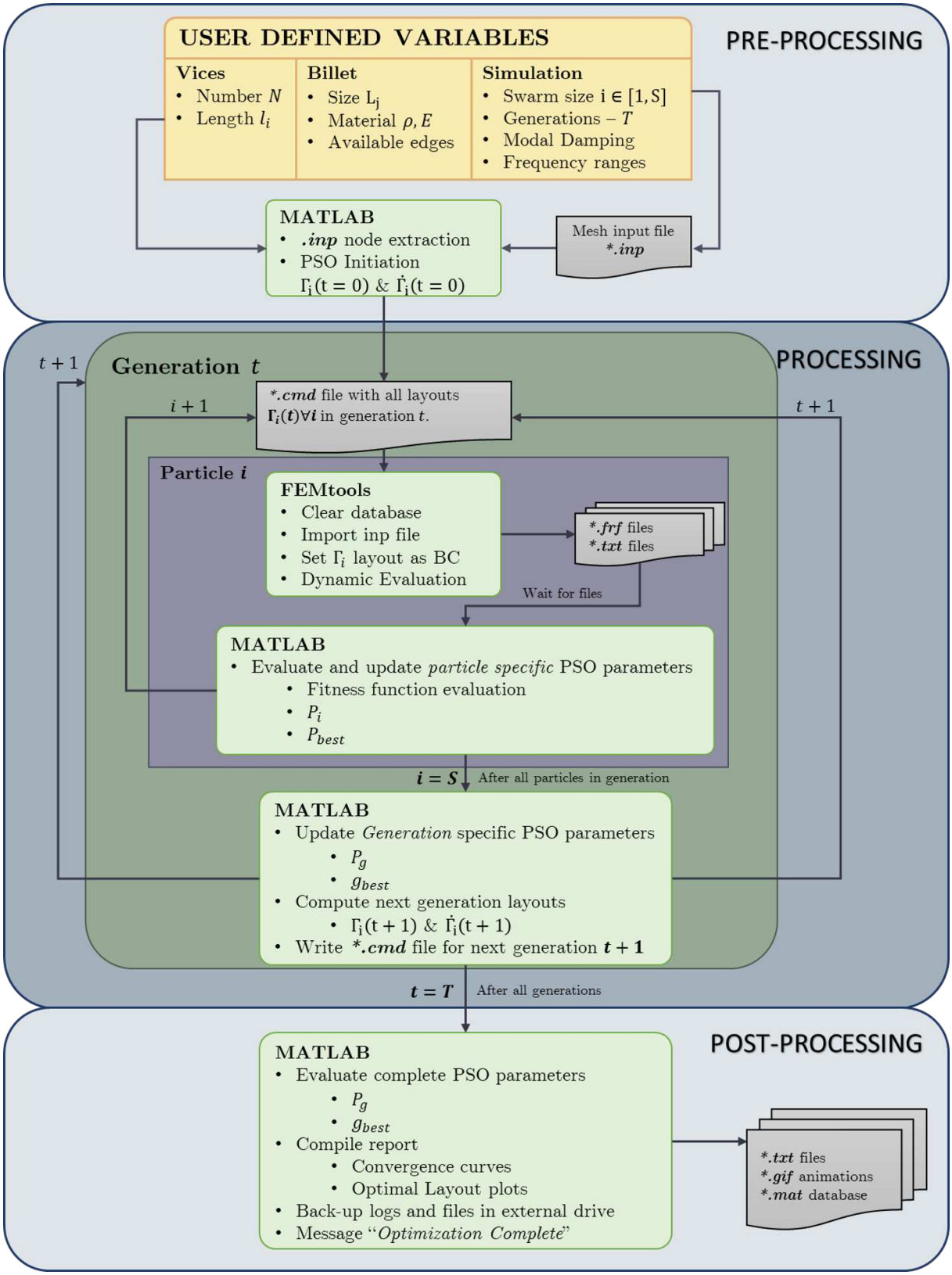

Figure 6: Flowchart of the optimisation process

well as the swarm parameters (number of particles and iterations), FRF frequency range and resolution. MATLAB then reads the mesh **.inp* file and generates a series of **.cmd* files which are executed by FEMTOOLS generating the successive simulations for each particle in the swarm. Once all the particles have been modelled and the FRFs extracted, MATLAB then compiles the information, extracts the fitness functions and updates the swarm's governing parameters which determine the next iteration. This cyclic process continues until all generations are evaluated and the program terminates by exporting a graphic report on the optimal layout reached and the associated convergence curve.

4 Numerical Simulations

The algorithm must be initially checked for consistency and convergence, ensuring that for a set of conditions, the same solution is found independent of the starting points for each particle. Alongside this, expansion of user defined variable and removal of any hard-coding in the program aims to broaden the optimisation script to a range of different workpiece geometries or constraints within the billet.

The exhaustive searches compare the PSO method to a simplified scenario, namely vice number reduction for both single and double vice layouts. A (500×700×60)mm billet is used as a starting point to check the program and run exhaustive searches. Firstly, a single vice search was confirmed by the PSO in 4 iterations to be in the expected position (centre of long edge). The dual vice search yields more interesting results.

4.1 Dual Vice Search

In this case, all combinations of two vice placements are evaluated using a full-factorial design. As per the combinatorial analysis of section 3.1 the total amount of layouts is inversely proportional to the spatial resolution, therefore to avoid running into a unmanageable simulation, the spatial resolution is set at 50mm intervals. For this case the superposition of vices is allowed (to obtain better surface plot definitions) resulting in a search space of $39^2 = 1521$ combinations. After running all these simulations and obtaining their FRFs, the fitness function is plotted as a surface contour graph, with the indexable vice positions in the XY plane and the resulting fitness in color based bands, as per figure 7.

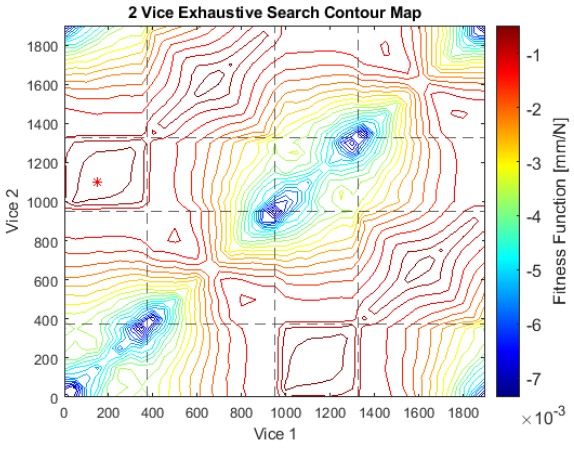

Figure 7: Dual vice search contour

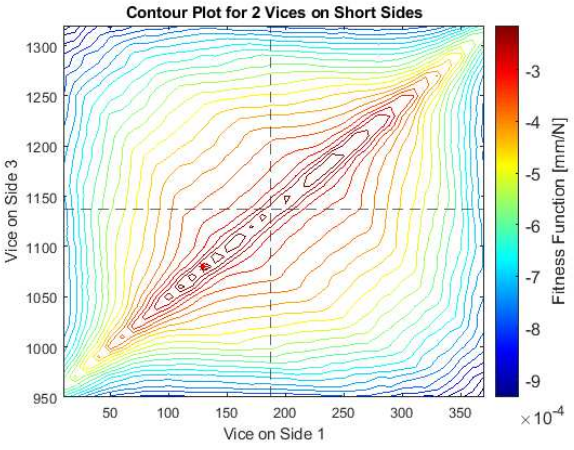

Figure 8: Short Sides Contour plot

Due to the symmetry of the system, the upper diagonal section is identical to the lower diagonal. The diagonal itself, corresponds to the single vice placement. The results at this stage, propose a maximum at coordinates of (150,1100) which has been highlighted in Figure 7 with *.

Once observed that the maximum was located in the quadrant where each vice is in either short sides of the billet, a subsequent search was performed for this area at a finer spatial resolution of 10mm. This allows to hone into the interested area and search for a more accurate optimal layout. The results, shown in Figure 8, indicate that the optimal layout in this case corresponds to coordinates (130,1080), which is the close to the one obtained in the coarser full space evaluation. This finer resolution effort, has highlighted the interesting behaviour along the main diagonal. In figure 8 the maximum has also been highlighted with $*$.

Remembering the definition for the indexable length, and its interpretation as a perimeter linear domain, the trajectory along the diagonal corresponds to vices starting at opposite corners (top-left and bottom-right) and moving towards the centre and back out again. The fitness functions presents a dip at the centre point of the billet (dotted line), which indicates that placing both vices at the centre of the edges does not necessarily equate to the best placement possible (under this particular evaluation method and fitness function).

Having inspected this dual vice layout definition, a PSO routine was launched to evaluate the effectiveness of the optimisation system. In this case, the PSO was defined with 30 particles and 50 generations. The optimal layout derived from the PSO was at coordinates (121.9 , 1077.5) and presented a marginally higher fitness function value than those obtained in either exhaustive search. The overall difference between the high resolution and PSO optimal are 8.1mm in vice #1 and 2.5mm in vice #2, which are under the spatial increments of the exhaustive search, and therefore this exact point was not scoped by any exhaustive search. Another interesting observation is that this PSO optimal does not lie exactly within the diagonal previously discussed, meaning that the vices are not placed at the same distances from the edges. In this case, vice #1 is placed around 5mm further towards the centre than vice #2, and therefore not contained within the strict definition if the main diagonal of Fig.8. The convergence curve for this PSO can be seen in Figure 9 while the layout definition of the PSO is plotted over the optimal of the exhaustive search for comparison in Figure 10. The resemblance of both layouts is evident and the fact that the PSO actually derived a better fitness function in half the amount of time is a good indication that the PSO system is working in a reliable manner.

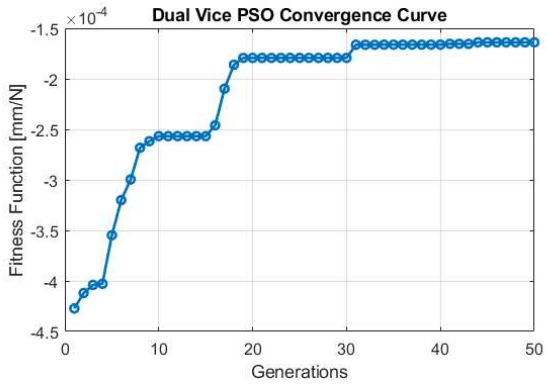

Figure 9: Dual vice PSO convergence curve

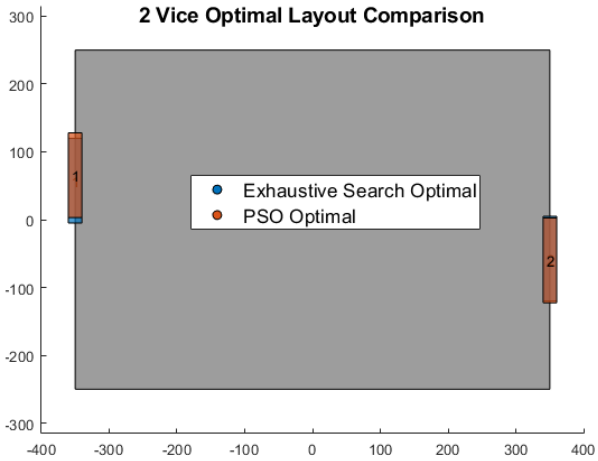

Figure 10: PSO optimal layout plotted over the exhaustive search optimal

5 Conclusions

The main purpose of this work is to establish the foundation for an optimisation program that can maximise the critical stable depth of cut for a minimally held workpiece. This is achieved by programming a PSO algorithm that automates the evaluation of different layouts in a FEA platform and compiles the results to define subsequent generations. This first stage looks at ensuring the PSO program is capable of consistently solving the system and contrasting these results against a known solution. In this benchmark study, the PSO program was able to deliver a better layout solution in less than half the time it took the exhaustive searches, but still requires extensive time computational power to find a solution. As complexity increases and more variables are added onto the solver, using exhaustive searches becomes impractical. These applications can range from evaluating different aspect ratio billets, increasing number of vices or incorporating a partially machined billet.

An important observation is the capability of expanding the fitness function to use the *lobing effect* in the SLDs and "climb" up a lobe to expand the MRR even further. This approach would require introducing geometric and modal parameters for the tooling and would considerably increase simulation times. A similar type of expansion on the system can be done on the fixturing side, given that most physical setups of this nature would need a frame or base to load the workpiece onto. The flexibility of this base will have a coupling effect and then multi-body assembly procedures are required. Both these aspects are proposed directions of development for this research.

Acknowledgements

This research was supported by GKN Aerospace and UK EPSRC grant EP/L016257/1.

References

[1] Fu R., Curley P., Higgins C., Kilic Z.M., Sun D., Murphy A. and Jin Y., 2022. Double-sided milling of thin-walled parts by dual collaborative parallel kinematic machines. *J. Mat. Proc. Tech.*, 299, p.117395.
[2] Boyle, I., Rong, Y. and Brown, D.C., 2011. A review and analysis of current computer-aided fixture design approaches. *Rob. and Computer-Integrated Manuf.*, 27(1), pp.1-12.
[3] Altintas Y 2012, *Manufacturing Automation: Metal Cutting Mechanics, Machine Tool Vibrations, and CNC Design* (Cambridge University Press)
[4] Schmitz T 2014, *Machining Dynamics* (Springer)
[5] Gameros A., Lowth S., Axinte D., Nagy-Sochacki A., Craig O. and Siller H.R., 2017. State-of-the-art in fixture systems for the manufacture and assembly of rigid components: A review. *Int. J. Mach. Tools Manuf.*, 123, pp.1-21.
[6] Liu, H., Wang, C., Li, T., Bo, Q., Liu, K. and Wang, Y., 2022. Fixturing technology and system for thin-walled parts machining: a review. *Front. Mech. Eng.*, 17(4), p.55.
[7] Wan XJ, Zhang Y, Huang XD. Investigation of influence of fixture layout on dynamic response of thin-wall multi-framed work-piece in machining. *Int. J. Mach. Tools Manuf.* 2013 Dec 1;75:87-99.
[8] Dou, J., Wang, X. and Wang, L., 2012. Machining fixture layout optimisation under dynamic conditions based on evolutionary techniques. *Int. J. of Prod. R.*, 50(15), pp.4294-4315.
[9] Rezaee Jordehi, A. and Jasni, J., 2013. Parameter selection in particle swarm optimisation: a survey. *J. Exp. & Theo. Art. Int.*, 25(4), pp.527-542.